Concawe
Environmental Science
for European Refining

Report

Report no. 15/20

Assessment of Photochemical Processes in Environmental Risk Assessment of PAHs

ISBN 978-2-87567-127-1

Assessment of Photochemical Processes in Environmental Risk Assessment of PAHs

E. Vaiopoulou (Concawe Science Executive)

This report was prepared by:

Tom Parkerton (ExxonMobil), Aaron Redman (ExxonMobil), Eleni Vaiopoulou

Under the supervision of:

E. Vaiopoulou (Concawe Science Executive)

At the request of:

Concawe's Environmental Management Group (EMG)

Acknowledgements to: Pete Bevel (whyistheskyblue.co), Michael Pidwirny (The University of British Columbia, CA) and Alastair Reid (MrReid.org) for providing permission to use Figures 1,2 and 5 respectively.

Brussels
August 2020

ABSTRACT

Petroleum substances may contain polyaromatic hydrocarbons (PAHs) that can interact with sunlight. These interactions can increase hazard, via photo-enhanced toxicity, and reduce exposure, due to photodegradation. These processes are not considered in the PETRORISK model, developed and used by Concawe for risk assessments of petroleum substances under REACH. To assess the role of photochemical reactions on hazard and exposure and resulting risks to aquatic life, available photodegradation and photoxicity data were used to calibrate hazard and multimedia exposure models for representative 3, 4, and 5-ring PAHs. These models were then used to calculate risks for a range of sunlight exposures in natural waters. Risks derived for these scenarios were then compared to the default case without light. Results showed risks with sunlight were similar to or lower than the no light scenario since the predicted enhancement in toxicity was mitigated by reduced exposure from photodegradation. Study findings indicate that neglecting light interactions in petroleum substance risk assessments do not preclude effective chemical management since risks are not increased.

KEYWORDS

polyaromatic hydrocarbons (PAHs); phototoxicity; photodegradation; petroleum substance risk assessment

INTERNET

This report is available as an Adobe pdf file on the Concawe website (www.concawe.eu).

CONTENTS

List of Figures

List of Tables

SUMMARY

Petroleum substances may contain polyaromatic hydrocarbons (PAHs) that can interact with sunlight. Hazard properties may be altered via photo-enhanced toxicity, while direct and indirect photodegradation processes may lead to decreased exposure. This potential interaction with sunlight is not considered by the Petrorisk modelling framework that has been developed and applied by Concawe for conducting environmental risk assessments of petroleum substances under REACH. The objective of this study is to assess the role of photochemical reactions on hazard and exposure and resulting implications for PAH risks to aquatic life.

To accomplish this goal, available photodegradation and photoxicity data were used to calibrate hazard and EUSES multimedia exposure models for a representative 3-ring (anthracene), two 4-ring (pyrene, fluoranthene) and a 5-ring (benzo(a)pyrene) PAH. These models were then used to calculate risk quotients to aquatic life for various regional scenarios in nutrient poor and rich natural waters during winter and summer seasons that reflect a range of sunlight exposures. Risk quotients from these scenarios were then compared to the default case that ignores light.

Results indicated that photodegradation rates were faster than biodegradation rates and of similar magnitude for all PAHs, except fluoranthene, which had a ten-fold slower rate. Analysis of photoxicity data indicated all PAHs exhibited a similar species sensitivity distribution when normalized to the combined PAH and daily ultraviolet light exposure metric of μW cm^{-2}μg L^{-1} . Resulting risk quotients for scenarios that included sunlight were similar to or lower than the no light case for the PAHs investigated, with the exception of fluoranthene, since the predicted enhancement in toxicity was effectively mitigated by reduced exposure due to photodegradation. This study indicates that neglecting light interactions in risk assessment for PAH containing petroleum substances does not preclude effective chemical management since risks are not significantly increased.

1. INTRODUCTION

1.1. BACKGROUND

Complex petroleum substances may contain PAHs that can interact with sunlight. These interactions can alter both hazard, as a result of photo-enhanced toxicity, and exposure, as a result of direct and indirect photodegradation processes. Currently, the potential interaction with sunlight is not considered by the Petrorisk modelling framework that has been developed and applied by Concawe for conducting generic environmental risk assessments of petroleum substances as required by the European Union REACH legislation [1]. Consequently, further analysis is warranted to assist Concawe in evaluating the technical basis for adjusting risk quotients (i.e. magnitude of potential assessment factors) for PAHs derived using Petrorisk where light interactions have not previously been considered.

1.2. OBJECTIVES

This project will use available data and models to assess the role of photochemical reactions on hazard and exposure assessment and resulting implications for PAH risk quotients to aquatic life. A key challenge in addressing photochemical reactions in generic risk assessment is the site-specific nature of these processes [2]. Since the generic local exposure scenario under REACH ignores the role of degradation processes in potentially mitigating substance exposures, the regional exposure scenario has been used in this study to evaluate how risk to the aquatic environment is altered by consideration of interactions with sunlight. This analysis will investigate a representative 3-ring (anthracene), two 4-ring (pyrene, fluoranthene) and 5-ring (benzo(a)pyrene) PAH that are subject to both phototransformation and photoenhanced toxicity.

The specific goals of this work were two-fold. The first aim was to determine the aquatic risk characterization ratios of selected PAHs for different generic model scenarios that reflect a range of light conditions in freshwater environments. The second objective was to compare risk characterization ratios for selected PAHs from this analysis to risk estimates that neglect sunlight to gain insights into the uncertainty associated with excluding such interactions in risk assessment.

2. MODELLING EXPOSURE WITH PHOTODEGRADATION

Direct photo-degradation involves the absorption of ambient light of a given wavelength by a substance and subsequent modification of the parent compound structure. The solar radiation reaching the earth's surface is > 290 nm, therefore substances that undergo direct photolysis must absorb light above this wavelength (**Figure 1**). This explains why compounds like monoaromatic or aliphatic hydrocarbons do not degrade via direct photolysis since the absorption spectra of these compounds do not overlap with that of the emission spectrum of sunlight [3].

The absorption of light from a solution is described by the Beer-Lambert Law:

$$Absorption\ (A) = log(I_\lambda / I_{o\lambda}) = \varepsilon_\lambda\ [C]\ L \qquad (1)$$

where $I_{o\lambda}$ is the incident light on a solution at wavelength λ, I_λ is the emergent light from the solution, [C] is the molar concentration of the substance, L is the path length of the solution in cm and ε_λ is the wavelength-dependent molar absorptivity of the compound.

Figure 1. Solar spectrum emitted from sun and reaching the earth's surface [Used by permission of Pete Bevel (2013)]

Source:https://images.app.goo.gl/UDWhW6k8Drr46jfz5

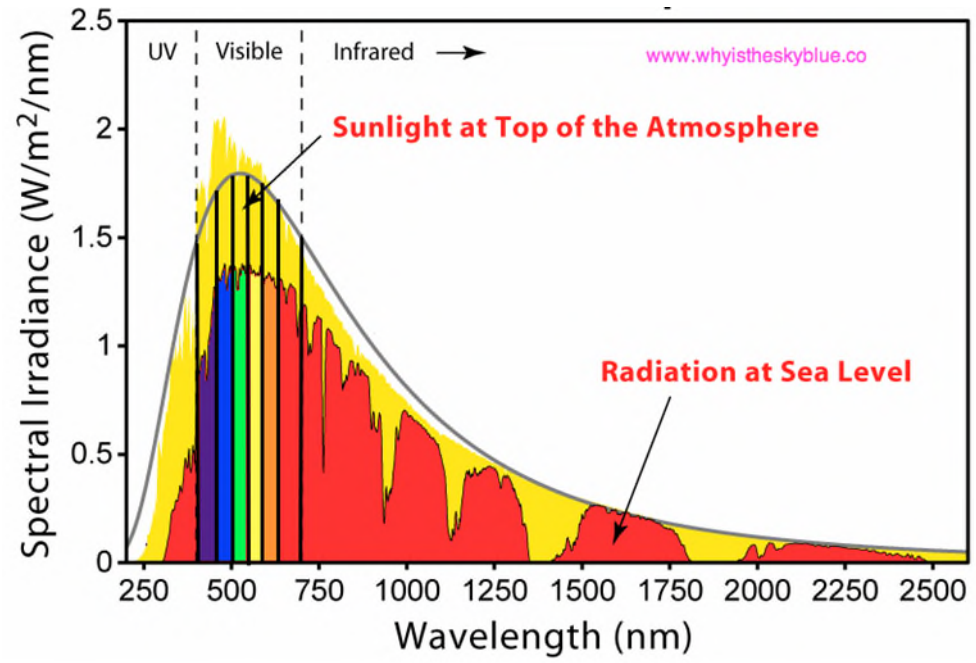

Calculating the first-order rate constant for direct photodegradation, also commonly referred to as photolysis, involves two steps. First, the photodegradation rate constant in "clean" water (k_o) is determined. There are two general methods for estimating this loss rate: from absorption spectra, or by extrapolation of lab studies [4,5]. Both approaches are described in the next sections.

2.1. CALCULATING SURFACE PHOTOLYSIS RATES FROM SUBSTANCE SPECIFIC ABSORPTION SPECTRA

The first method involves using the substance absorption spectrum over the ambient solar spectrum ultraviolet-visible range (290-800 nm), utilizing an experimentally determined quantum yield and calculated solar irradiance at the water surface which varies with latitude and time of year (**Figure 2**).

Using this approach, k_o is calculated as follows:

$$k_o = \varphi \sum_{\lambda=290}^{\lambda=800} \varepsilon_\lambda \; L_{o,\lambda} \qquad (2)$$

where:

k_o = photodegradation rate at water surface d^{-1}

φ= reaction quantum yield (mol einstein^{-1}), i.e. the quantum yield (φ) is a measure of the photochemical reaction efficiency expressed as mols of substance that is phototransformed per mol of photons absorbed

ε_λ = molar absorptivity at wavelength λ (L mol^{-1} cm^{-1})

$L_{o\lambda}$ = average diurnal surface light at wavelength λ (millieinsteins $cm^{-2}d^{-1}$)

The product on the right side of this equation represents the rate at which light is absorbed. For PAHs, absorption occurs largely at wavelengths in the ultraviolet light (UV-B, 280 to 315 nm and UV-A, 315 to 400 nm) region of the spectrum. However, not all absorbed light results in molecular transformations as other mechanisms allow excited molecules to release the absorbed light energy. The quantum yield (φ) defines the efficiency at which absorbed light results in a molecular structural transformation.

Figure 2. Monthly irradiance at the equator, 30, 60, and 90° N latitudes [Used by permission of Michael Pidwirny (2006)]

Source: http://www.physicalgeography.net/fundamentals/6i.html

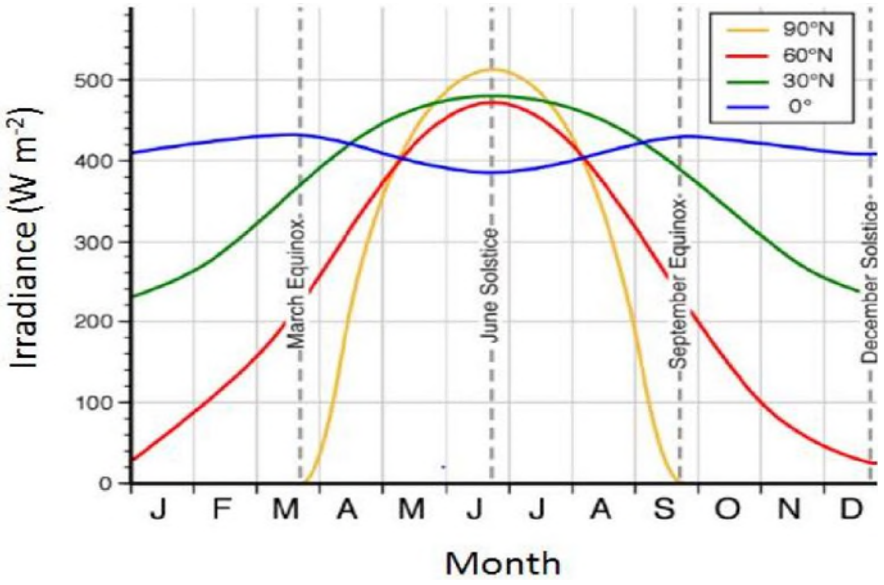

Light absorption for representative PAH compounds was experimentally determined using a Hewlett-Packard 8453 diode array UV-VIS spectrophotometer using a 1 cm quartz cell, a scan time of 0.5 seconds, and resolution of 2 nm. Absorption spectra were obtained using a 100ppm concentration of each substance dissolved in octanol with results shown in **Figure 3**. Molar absorptivity's for different wavelength intervals were then determined by re-arrangement of equation (**Equation 1**).

For compounds that are rapidly photodegraded, a higher light intensity reflecting afternoon conditions may provide a more accurate estimate of photodegradation rates in the field [2]. However, diurnal light intensities averaged over a 24 hour period have been used to provide conservative estimates of photolysis rates in this screening analysis. Since light intensity at the water surface varies over time, two scenarios will be considered reflecting mid-summer conditions and mid-winter conditions at 40ºN latitude that correspond to a location comparable to Madrid, Spain. As indicated in **Figure 2**, the proposed solar light intensities corresponding to this location (i.e. falling below green line in **Figure 2**) are conservatively representative of the range of light incident at most latitudes within Europe and are thus generalizable [3].

Tables of $L_{o,\lambda}$ have been tabulated by USEPA for different latitudes and seasons [6]. Average irradiances during both summer and winter periods at 40º N latitude were used to assess seasonal influence. Estimated rates at which surface light is absorbed by the representative PAHs are summarized in **Table 1** with detailed calculations included in **Appendix 1**.

Table 1. Rate of light absorption for selected PAHs

Test Substance	Summer $\Sigma\ \varepsilon_\lambda\ L_{o,\lambda}\ (h^{-1})$	Winter $\Sigma\ \varepsilon_\lambda\ L_{o,\lambda}\ (h^{-1})$
Anthracene	132	41
Fluoranthene	160	48
Pyrene	86	23
Benzo(a)pyrene	332	105

A compilation of empirically derived quantum yields for the substances evaluated in this study is provided by Fasnacht and Blough [7]. Results are summarized in **Table 2** along with calculated photolysis rates derived using **equation 2**. Estimated photolysis rates are on the same order of magnitude for anthracene, pyrene and benzo(a)pyrene but are more than an order of magnitude slower for fluoranthene. Rates are also approximately three times faster during summer than winter.

Table 2. Quantum yields for selected PAHs and estimated water surface photolysis rates

Test Substance	Quantum Yield (φ)	Summer $K_o\ (hr^{-1})$	Winter $K_o\ (hr^{-1})$
Anthracene	3.0×10^{-3} (λ = 366 nm) 4.2×10^{-3} (polychromatic)*	0.55	0.17
Fluoranthene[a]	1.2×10^{-4} (λ = 313 nm) 2.0×10^{-6} (λ = 366 nm) 3.2×10^{-5} (polychromatic)*	0.0051	0.0015
Pyrene[b]	2.0×10^{-3} (λ = 313 nm) 2.8×10^{-3} (λ = 313 nm) 2.1×10^{-3} (λ = 366 nm)*	0.18	0.05
Benzo(a)pyrene[c]	8.9×10^{-4} (λ = 313 nm) 5.4×10^{-4} (λ = 366 nm) 5.4×10^{-3} (polychromatic)	0.33	0.10

* value selected for calculation
a literature values at 313 and 366 nm reported by Mills et al. 1985 [8]
b since maximum absorption occurs near 316 nm (**Figure 3**) the mean value at λ=313 nm is used
c due to the discrepancy in reported results a value for φ = 1×10^{-3} is assumed

Figure 3. Absorption spectra of selected PAHs in octanol.

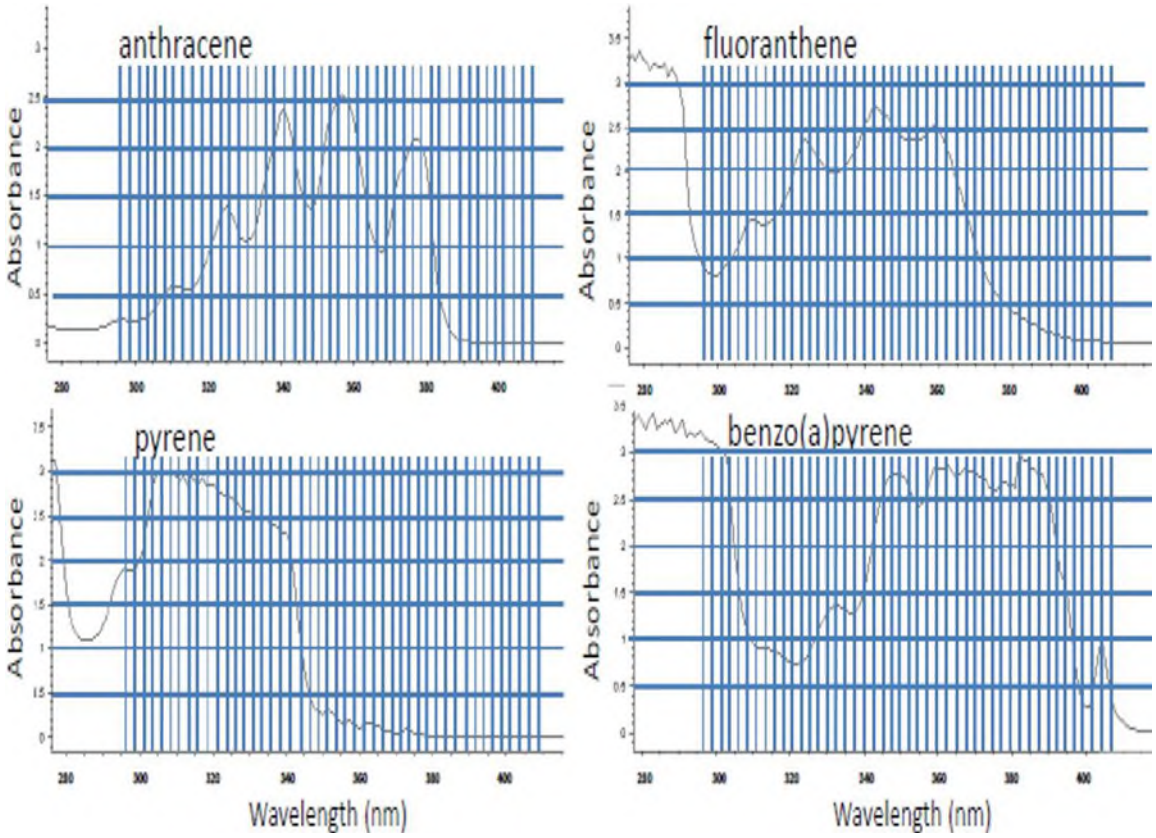

2.2. CALCULATING SURFACE PHOTOLYSIS RATES FROM LAB TESTS

A second approach to determine surface photolysis rates involves extrapolation of empirical laboratory measurements at a given light intensity to the solar light intensity for the field scenario of interest:

$$k_o = 1.33 \frac{I_o}{I_{lab}} k_{lab} \quad (3)$$

where:

$I_o =$ light intensity at water surface in the field (Watts m^{-2})

$I_{lab} =$ light intensity used to estimate photo-degradation rate in clean lab water (Watts m^{-2})

$k_{lab} =$ photodegradation rate in clean lab water (d^{-1})

A compilation of lab-derived photolysis rates is presented in **Table 3**. Data for phenanthrene are also included as several investigations have been reported this compound. Some studies included in this Table have examined the role that dissolved organic carbon (DOC) may play in mitigating photolysis rates. Results suggest DOC can reduce laboratory derived rates but generally not more than a factor of two. Comparison of **Table 2** and **3** suggests surface photolysis rates derived using the two approaches yield similar results for anthracene, pyrene and benzo(a)pyrene. A greater discrepancy is observed for fluoranthene with lab measurements yielding an order of magnitude faster rate. This discrepancy may reflect the greater uncertainty in the quantum yield for fluoranthene which appears to be wavelength-dependent (**Table 2**).

Table 3. Lab derived photolysis rates and extrapolated water surface photolysis rates

Substance	I_{lab} (W m^{-2})	k_{lab} (h^{-1})	Comments	Reference	k_o, summer (h^{-1})[a]	k_o, winter (h^{-1})[a]
Anthracene	1018	0.92		Mills 1985[8]	0.46	0.20
Fluoranthene	1018	0.033		Mills 1985	0.016	0.007
	1450	0.24	milli-Q water	Xia. 2009[9]	0.084	0.036
	1450	0.39	milli-Q water + DOC=1.25 mg/L	"	0.136	0.059
	1450	0.15	milli-Q water + DOC=14.6 mg/L	"	0.052	0.023
				median =	0.068	0.030
Pyrene	1018	1.02		Mills 1985	0.51	0.22
	*	16.1	Oxygenated	Clark 2007[10]	0.54	0.23
	*	2.5	de-oxygenated	"	0.08	0.04
	1018	2.52	milli-Q water	Jacobs 2009[11]	1.25	0.54
	1018	1.41	river water, DOC=6.7 mg/L	"	0.70	0.30
	1018	1.08	river water, DOC=9.3 mg/L	"	0.54	0.23
	1450	1.91	milli-Q water	Xia. 2009	0.67	0.29
	1450	2.1	milli-Q water + DOC=1.25 mg/L	"	0.73	0.32
	1450	0.92	milli-Q water + DOC=14.6 mg/L	"	0.32	0.14
				median =	0.54	0.23
Benzoapyrene	1018	1.17		Mills 1985	0.58	0.25
Phenanthrene	1018	0.083		Mills 1985	0.041	0.018
	1018	0.055	milli-Q water	Jacobs 2009	0.027	0.012
	1018	0.071	river water, DOC=6.7 mg/L	"	0.035	0.015
	1018	0.041	river water, DOC=9.3 mg/L	"	0.020	0.009
	*	1.8	deionized water	de Bruyn 2012[12]	0.060	0.026
	*	0.9	deionized water + DOC= 1 mg/L	"	0.030	0.013
	*	0.36	deionized water + DOC= 10 mg/L	"	0.012	0.005
				median =	0.030	0.013

a average summer and winter irradiance was assumed to be 351 and 165 W m^{-2} at 40°N latitude, respectively based on data provided by Mills et al. 1985 [8]. These values were used as inputs to **equation 3** to adjust lab reported rates to reflect these light exposures.

* irradiance values were not provided but authors provide scaling factor of 30 to correct results to reflect sunlight; this correction factor has been used to estimate the photolysis rate in summer; winter rates are estimated based on differences in light irradiance during summer and winter periods described above.

2.3. CALCULATING AVERAGE PHOTOLYSIS RATES FOR DIFFERENT SEASONS AND WATER BODIES

Once the photodegradation rate at the surface is determined, the next step is then to translate this estimate into a depth-integrated value. To estimate the photodegradation rate over the water column the following equation is used:

$$k_{photo} = k_o \frac{1-e^{[-\alpha_{\lambda \max} Z]}}{\alpha_{\lambda \max} Z} \quad (4)$$

where:

k_{photo} = photodegradation rate over water column used in exposure modelling (d^{-1})

$\alpha_{\lambda max}$ = light extinction coefficient in water body at wavelength corresponding to maximum light absorption by substance (m^{-1})

Z = depth of water body (m)

The term $\alpha_{\lambda max}$ determines the extent to which the ambient surface light is attenuated in the water column which has been shown to be a function of chlorophyll a, DOC and total suspended solids in the water column. Correlations have been used to calculate the light extinction coefficient for each of the four model PAHs for both an oligotrophic and eutrophic water body based on the equation provided by Chapra et al. [4].

$$\alpha_{\lambda max} = 1.4 \left[\alpha_{o,\lambda max} + \alpha_{chl,\lambda max} \text{ Chl a} + \alpha_{DOC,\lambda max} \text{ DOC} + \alpha_{TSS,\lambda max} \text{ TSS} \right] \quad (5)$$

where:

Chl a = chlorophyll a concentration (mg/L)
DOC = dissolved organic carbon (mg/L)
TSS = total suspended solids (mg/L)

The coefficients for **equation 5** are provided in **Table 4** based on λ_{max} for each PAH that was estimated from **Figure 1**. The assumed water quality parameters that are also required inputs for the two different water body types are provided in **Table 5**.

Table 4. Coefficients for determining light extinction as a function of wavelength

Substance	λ_{max} (nm)	α_o	α_{chl}	α_{DOC}	α_{TSS}
Anthracene	355	0.0379	55	2.12	0.35
Fluoranthene	340	0.0561	58	3.50	0.35
Pyrene	310	0.1127	66	5.47	0.35
Benzo(a)pyrene	380	0.0220	46	1.96	0.35

Table 5. Water quality parameters assumed for different water bodies

Water Type	Chlorophyll a (mg/L)	Dissolved Organic Carbon (mg/L)	Total Suspended Solids (mg /L)
Oligotrophic	0.002	0.2	1
Eutrophic	0.04	2.0	10

The estimated extinction coefficient derived for each compound and water body can be used to delineate the depth of the photic zone at which ambient light intensity in the water column that is preferentially absorbed by the substance falls below a defined percentage of the incident light at the water surface. For example, the depth at which 5% of the light reaches can be estimated by:

$$Z_{0.05} = \frac{3}{\alpha_{\lambda max}} \quad (6)$$

Application of this equation can be used to define the depth range of which phototransformation processes are a relevant consideration. **Equations 4** through **6** have been applied in conjunction with indicative surface photolysis rates deduced from **Tables 2** and **3** to determine photodegradation rates for different seasons and water bodies for each representative PAH. A depth of 3 m has been assumed based on the default EUSES depth used for regional exposure assessments. Results are summarized in **Table 6**. Estimated $\alpha_{\lambda max}$ values range from 1.29 to 24.1 m^{-1} and bracket the typical value recommended for freshwater of 5 m^{-1} [13]. For comparison the default biodegradation rates predicted by the BioHCwin HCBioWin model [14] and used as input to Concawe Petrorisk model multi-media exposure assessments are also provided. Observed photodegradation rates are orders of magnitude faster than predicted biodegradation rates even during the winter period in eutrophic water bodies where light intensity and water transparency are reduced.

Table 6. Influence of season and water body type on light extinction, penetration depth and average photolysis rates for selected PAHs.

Substance	Season	Water Type	$\alpha_{\lambda max}$ (m^{-1})	$Z_{0.05}$ (m)	$k_{0,surface}$ (h^{-1})	k_{photo} (d^{-1})	k_{biodeg} (d^{-1})
Anthracene	Summer	Oligotrophic	1.29	2.32	1.0	6.069	0.00563
	Winter	Oligotrophic	1.29	2.32	0.3	1.821	
	Summer	Eutrophic	14.0	0.21	1.0	0.573	
	Winter	Eutrophic	14.0	0.21	0.3	0.172	
Fluoranthene	Summer	Oligotrophic	1.71	1.75	0.03	0.139	0.00363
	Winter	Oligotrophic	1.71	1.75	0.01	0.046	
	Summer	Eutrophic	18.0	0.17	0.03	0.013	
	Winter	Eutrophic	18.0	0.17	0.01	0.004	
Pyrene	Summer	Oligotrophic	2.36	1.27	0.30	1.014	0.00245
	Winter	Oligotrophic	2.36	1.27	0.10	0.338	
	Summer	Eutrophic	24.1	0.12	0.30	0.1	
	Winter	Eutrophic	24.1	0.12	0.10	0.033	
Benzo(a)pyrene	Summer	Oligotrophic	1.20	2.50	0.50	3.246	0.00164
	Winter	Oligotrophic	1.20	2.50	0.15	0.974	
	Summer	Eutrophic	11.7	0.26	0.50	0.342	
	Winter	Eutrophic	11.7	0.26	0.15	0.103	

The analysis presented in the previous sections has specifically attempted to quantify direct photolysis. However, photodegradation can also proceed via two indirect mechanisms: 1) light absorbed by a sensitizer transfers this energy to a substance resulting in a transformation or 2) photo-chemically derived reactive species, such as hydroxyl radicals, react with the substance. While methods are available to quantitatively assess direct photodegradation rates for use in generic modelling, standard procedures are not available to quantify the rate of indirect photolysis [13]. Thus, for the purpose of this screening analysis we have considered only direct photolysis. This assumption provides a conservative basis for evaluating the role of photodegradation on exposure assessment particularly for eutrophic water bodies that contain higher concentrations of chromatophores that can serve as potential sensitizers [3].

2.4. ASSESING THE INFLUENCE OF PHOTODEGRADATION ON REGIONAL EXPOSURE ASSESSMENT

To gain initial insights into the role that both photolysis and biodegradation loss processes play in reducing exposure to the selected PAHs, at one compartment, steady-state mass balance model can be applied:

$$W = Q\, C_{water} + [\, k_{photo} + k_{biodeg} \,]\, C_{water}\, V \qquad (7)$$

where:

W = emission rate of substance into water body (kg/d)
Q = water flow ($m^3\ d^{-1}$)
V = water volume (m^3)
C_{water} = steady state concentration of test substance in water (kg m^3= g L^{-1})
and k_{photo} and k_{biodeg} represent first order loss rates (d^{-1}) defined in **Table 6.**

Solving equation (7) for C_{water} yields:

$$C_{water} = \frac{W}{Q + [k_{photo} + k_{biodeg}]\, V} \qquad (8)$$

The first term in the denominator reflects the dilution rate of the discharge while the second term quantifies the collective role of abiotic and biotic degradation processes in reducing exposures in the water. In the EUSES regional model, the volume and flow of regional freshwater is 3.6 x $10^9\ m^3$ and 9.6 x $10^2\ m^3\ s^{-1}$ (= 8.3 x $10^7\ m^3\ d^{-1}$). This equates to a residence time in the regional water compartment of 43 days. Assuming an emission discharge of 10 T/yr and no degradation, the estimated water concentration is therefore 0.33 µg/L. **Equation 8** can be further applied with the EUSES regional defaults and photo and biodegradation rates provided in **Table 6** as inputs. Results of these calculations are provided in **Table 7** and indicate that with the exception of fluoranthene, predicted concentrations are generally reduced by more than 90% when degradation is included. Since the photolysis rate of fluoranthene is slower, the extent to which exposure is reduced is lower with a 22% reduction predicted during winter in a eutrophic water body and a 84% reduction in summer for an oligotrophic water body. This analysis indicates that the residence time in the regional water compartment included within EUSES is sufficient to allow much of emitted discharge of the selected PAHs to be photodegraded in a regional scenario. This simple analysis suggests ignoring direct photolysis rates as done in the Petrorisk model may significantly overstate exposure for PAHs that are susceptible to phototransformation.

It is also important to point out that the default biodegradation rates obtained using HCBioWin are likely to be overly conservative. For example, in the study by Kot-Wasik et al. 2004 [15] in which benzo(a)pyrene was incubated in natural river and pond water in the dark, reported biodegradation half-lives of 27 to 47 days (ca. 0.0187 d^{-1}) were reported. This rate is more than an order of magnitude higher than the prediction in **Table 6** and if used in the screening calculations described above would yield predicted concentrations equal to 0.18 µg/L which corresponds to a 45% reduction in exposure concentration versus the no degradation scenario.

Table 7. Predicted steady-state water concentrations computed using a one-compartment mass balance model incorporating first-order photodegradation and biodegradation loss processes.

Substance	Season	Water Type	Predicted C_{water} Photo+Biodeg (µg L^{-1})	Predicted C_{water} Biodeg Only (µg L^{-1})	% Reduction with photo degradation
Conserved Substance	All	All	0.33	0.33	NA
Anthracene	Summer	Oligotrophic	1.2E-03	2.7E-01	99.5
	Winter	Oligotrophic	4.2E-03	2.7E-01	98.4
	Summer	Eutrophic	1.3E-02	2.7E-01	95.3
	Winter	Eutrophic	3.6E-02	2.7E-01	86.3
Fluoranthene	Summer	Oligotrophic	4.6E-02	2.9E-01	84.0
	Winter	Oligotrophic	9.9E-02	2.9E-01	65.2
	Summer	Eutrophic	1.7E-01	2.9E-01	38.9
	Winter	Eutrophic	2.2E-01	2.9E-01	22.2
Pyrene	Summer	Oligotrophic	7.4E-03	3.0E-01	97.5
	Winter	Oligotrophic	2.1E-02	3.0E-01	93.0
	Summer	Eutrophic	6.1E-02	3.0E-01	79.6
	Winter	Eutrophic	1.3E-01	3.0E-01	57.8
Benzo(a)pyrene	Summer	Oligotrophic	2.4E-03	3.1E-01	99.2
	Winter	Oligotrophic	7.6E-03	3.1E-01	97.5
	Summer	Eutrophic	2.1E-02	3.1E-01	93.2
	Winter	Eutrophic	6.1E-02	3.1E-01	80.2

Figure 4. Regional predicted environmental concentrations (relative to k_{biodeg} case) from EUSES (based on 10 T/yr emission) for individual PAH as a function of overall first order loss rate (k_{photo} + k_{biodeg}).

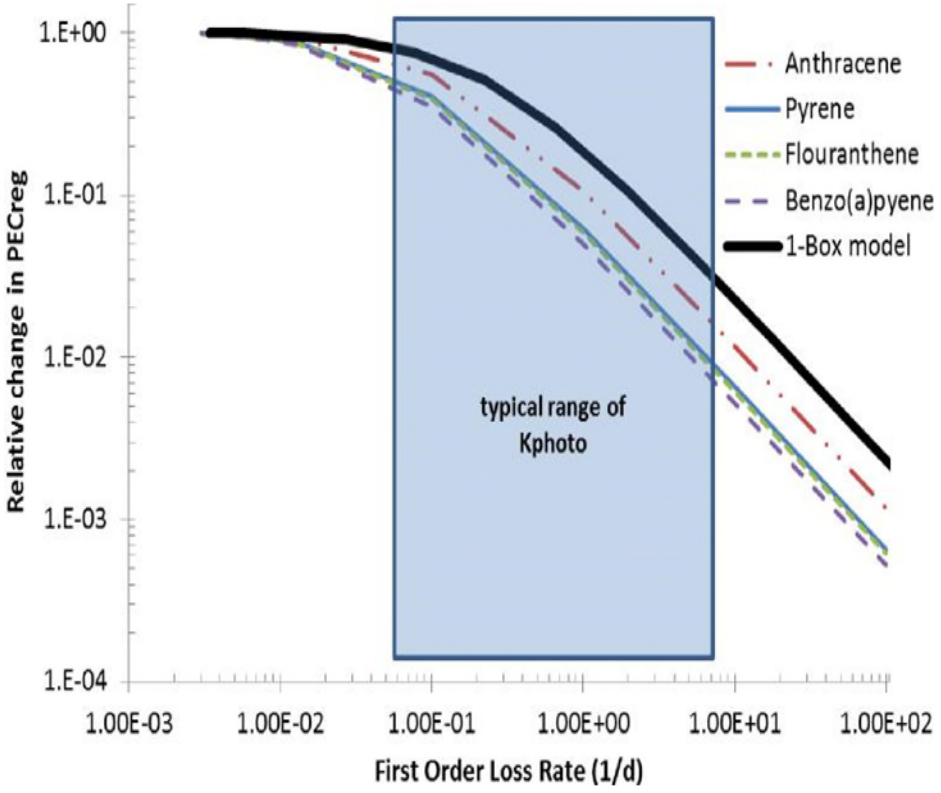

Simulations presented in **Table 7** were run in EUSES to model the fate of the four PAHs evaluated in this study using a common exposure assessment framework. EUSES is the basis of the Concawe Petrorisk risk assessment tool [1], which was designed to model complex petroleum substances and is used in this work to investigate the influence of incorporating photodegradation on predicted exposures (see next section). Simulations were performed assuming regional emissions of 10 T/yr into water with and without photolysis (**Table 8**). Overall loss rates can vary from ~ 10^{-3} d^{-1} for typical biodegradation rates, and from 0.01 to 10 d^{-1} for scenarios with photolysis included (**Table 7**). The results are discussed in relative terms since exposure predictions scale linearly to the emission rate.

EUSES model predictions (**Figure 4**) illustrate the expected behavior of these PAH as a function of the overall first order loss rate (e.g., k_{biodeg}+k_{photo}). Concentrations at low loss rates (0.001 to 0.01 d^{-1}) are relatively invariant due to the retention time in this system, i.e. 43 days. This is confirmed with the simple one-box model discussed above (bold line, **Figure 4**). This indicates that regional exposure concentrations for these constituents are dictated by dilution from advection out of the regional compartment before biodegradation losses can significantly contribute to the substance mass balance. Consistent with the one-box model simulations, implementation of photodegradation in the model calculations results in much lower predicted environmental concentrations (PECs) than the conserved substance base case (i.e. no photolysis or biodegradation). Three of the PAHs demonstrated substantial removal (>80%) in oligotrophic systems, and

generally removal >60% in eutrophic systems. Fluoranthene demonstrated lower removal (6-70%) consistent with the lower photodegradation rates. The extent of removals derived from EUSES exposure predictions when photodegradation is included are lower than the 1-box model since EUSES includes additional removal processes (e.g., Sewage Treatment Plant (STP), volatilization, settling) that lower the absolute value of PECs thereby reducing the contribution from photodegradation to overall removals (e.g. compare **Table 7** to **Table 8**). However, the trends are the same showing rapid decline in concentrations with increasing loss rate (**Figure 4**).

The simulations demonstrate that photolysis significantly affects the fate of PAHs in the environment. Removal ranges from approximately a factor of two to nearly a factor of 100 depending on the water quality conditions. At low loss rates (<0.01d^{-1}) the residence time in the system is too short for these processes to materially impact the concentrations. For the PAHs in the scenarios studied here, most have photolysis rates >0.01 d^{-1} for most conditions. The following section will evaluate the relative impact of UV-light exposure on the aquatic hazard of the four study PAHs.

Table 8. Predicted environmental concentrations (PECs) from EUSES for a conserved chemical (e.g., no loss), with only biodegradation, and including both biodegradation and photodegradation processes.

Substance	Season	Water Type	k_{photo} (1/d)	k_{biodeg} (1/d)	Total Loss Rate (1/d)	PEC conserved[a] (mg/L)	PEC biodeg (mg/L)	PEC photo+ biodeg (mg/L)	% Reduction with photodeg
Anthracene	Summer	Oligotrophic	6.1E+00	5.6E-03	6.1E+00	3.87E-02	3.69E-02	7.33E-04	98.0
	Winter	Oligotrophic	1.8E+00	5.6E-03	1.8E+00	3.87E-02	3.69E-02	2.38E-03	93.6
	Summer	Eutrophic	5.7E-01	5.6E-03	5.8E-01	3.83E-02	3.66E-02	6.49E-03	82.2
	Winter	Eutrophic	1.7E-01	5.6E-03	1.8E-01	3.83E-02	3.66E-02	1.52E-02	58.4
Fluoranthene	Summer	Oligotrophic	1.4E-01	3.6E-03	1.4E-01	5.83E-02	5.49E-02	1.71E-02	68.8
	Winter	Oligotrophic	4.6E-02	3.6E-03	5.0E-02	5.83E-02	5.49E-02	3.14E-02	42.9
	Summer	Eutrophic	1.3E-02	3.6E-03	1.7E-02	5.44E-02	5.14E-02	4.26E-02	17.1
	Winter	Eutrophic	4.0E-03	3.6E-03	7.6E-03	5.44E-02	5.14E-02	4.84E-02	5.8
Pyrene	Summer	Oligotrophic	1.0E+00	2.5E-03	1.0E+00	6.22E-02	6.00E-02	3.78E-03	93.7
	Winter	Oligotrophic	3.4E-01	2.5E-03	3.4E-01	6.22E-02	6.00E-02	9.95E-03	83.4
	Summer	Eutrophic	1.0E-01	2.5E-03	1.0E-01	6.06E-02	5.84E-02	2.40E-02	58.8
	Winter	Eutrophic	3.3E-02	2.5E-03	3.5E-02	6.06E-02	5.84E-02	3.95E-02	32.3
Benzo(a)pyrene	Summer	Oligotrophic	3.2E+00	1.6E-03	3.2E+00	5.22E-02	5.02E-02	6.84E-04	98.6
	Winter	Oligotrophic	9.7E-01	1.6E-03	9.8E-01	5.22E-02	5.02E-02	2.17E-03	95.7
	Summer	Eutrophic	3.4E-01	1.6E-03	3.4E-01	3.88E-02	3.76E-02	5.15E-03	86.3
	Winter	Eutrophic	1.0E-01	1.6E-03	1.0E-01	3.88E-02	3.76E-02	1.33E-02	64.7

3. MODELLING PHOTOTOXICITY

The objectives of this next section are to: 1) briefly explain the mechanistic basis of the enhanced toxicity of certain PAHs when combined with sunlight; 2) discuss dose metrics that can be used to characterize and model phototoxicity; 3) present an analysis framework that can be used to interpret available toxicity data sets using these metrics; 4) illustrate application of this framework for the four PAHs included in this study; 5) use results of this preliminary analysis to characterize the hazard associated with photoenhanced toxicity for the different exposure modelling scenarios discussed in the previous section.

3.1. MECHANISTIC OVERVIEW

The account describing the unexpected discovery that sunlight interacts with anthracene to enhance toxicity to aquatic organisms has been documented [16]. This early work lead to the finding that toxicity was dependent on the amount of anthracene in the organism and the UV-A light exposure (λ = 320–400 nm). These empirical observations are consistent with the Bunsen-Roscoe law of photochemical reciprocity which posits that photoactivated toxicity should be related to the product of PAH concentration and UV light exposure. The underlying mechanism describing phototoxicity is attributed to oxidative tissue damage caused by reactive oxygen species that are formed following absorption of UV light wavelengths by the substance that is accumulated in the organism [17]. This understanding is often incorporated into the design of phototoxicity studies by first exposing organisms to aqueous exposure concentrations of the test substance under dark conditions so organisms can bioconcentrate the test material followed by a subsequent period of known UV-exposure.

Past work has shown that the potential for PAH phototoxicity can be related to quantum structural descriptors such as the homo-lumo (highest occupied molecular orbital-lowest unoccupied molecular orbital) gap [18]. This model, which was derived using Daphnia magna acute toxicity data, predicts that the potential for phototoxicity peaks at a homo-lumo gap (HLG) of ca. 7.2 electron volts (eV) and then decreases for structures spanning a range from ca. 6.8 to 7.6 eV. In a more recent study further toxicity data are provided demonstrating that this simple model has utility for predicting photoxicity in algae [19]. The HLG for anthracene, fluoranthene, pyrene and benzo(a)pyrene, selected as representative PAHs in this study, is 7.3, 7.7, 7.2 and 6.8 eV respectively. Hence, using this model all of these substances are predicted to be within the range where phototoxicity is expected. In contrast, many PAHs that are prominent constituents in petroleum substances, such as fluorene and phenanthrene, fall outside this range. Thus, there is a wider range of PAHs that are susceptible to photodegradation that do not pose a phototoxicity hazard. Further, methyl substitution of the parent PAH appears to have only a minor influence on the magnitude of the HLG so this generalization applies to both parent and alkylated structures (e.g. methyl pyrene is subject to both photoxicity and photodegradation while methyl phenathrene is expected to be influenced by only photodegradation processes) [20].

3.2. DOSE METRICS FOR PHOTOTOXICITY

A common approach to express the results of phototoxicity tests is to relate the time required to cause a 50% response (LT_{50}) to the product of accumulated tissue concentration and the UV light intensity [21, 22]. This dose metric is often expressed in terms of µW cm^{-2} µg $g_{tissue(wet)}$-1. Alternatively, this metric can be expressed in terms of cumulative light energy in Joules (i.e. J cm^{-2} µg $g_{tissue}-1$) by multiplying by the duration of the UV exposure and relevant conversion factors (Diamond et al. 2006). For example, given a 12 h exposure at a UV irradiance of 500 µW cm^{-2} the resulting cumulative light energy would be 7.2 J cm^{-2} i.e. = 500 µW cm^{-2}x 1 W / 10^6 µW x 12 h x 60 min / h x 60 sec/min, where Joules = Watt-sec). If the dose metric used to characterize the LT_{50} discussed above is divided by the bioconcentration factor (BCF) for the substance then test results can be expressed in units of µW cm^{-2} µg L^{-1}. Often the empirical substance specific BCF for the test organism under investigation is reported or can be calculated from data presented in such studies.

While expressing photoxicity in terms of a tissue residue is preferable, if one assumes that the bioconcentration factor is independent of exposure concentration, as is typically assumed for organic chemicals tested below the solubility limit, then photoxicity should also scale to the reported effects concentration in water, e.g. LC_{50}. This is illustrated by the algal toxicity dataset for anthracene reported by Gala and Geisy [23] that is shown in **Table 9**.

Table 9. Acute effects of anthracene on algal growth at different UV-A light exposures after 22 h (Table adapted by [23])

I_{UVA} (µW cm^{-2})	$EC_{50,uva}$ (µg L^{-1})	I_{UVA} x $EC_{50,uva}$ (µW cm^{-2})µg L^{-1})
125	37.4	4675
218	12.1	2638
406	5.3	2152
410	6.6	2706
765	3.9	2984

As expected, these results show that the observed toxicity is inversely proportional to UV light intensity. From this study a mean dose metric value of 3031 µW cm^{-2} µg L^{-1} can be derived to characterize phototoxicity of anthracene to this test species. If this value is normalized to the exposure duration of UV light (22/24 h) then a 24 h normalized value of 2778 µW cm^{-2} µg L^{-1} is obtained. In cases where toxicity endpoints are reported following multiple days of diurnal UV exposure the dose estimate is adjusted for the light dark cycle. For example, if the dose metric of 1000 µW cm^{-2} µg L^{-1} is derived from a 96 hr study where a 12 h UV light: 12 h dark period was used the adjusted value used to characterize this toxicity study would be 500 µW cm^{-2} µg L^{-1}. This approach can be applied in analysis of other phototoxicity datasets that are deemed of acceptable quality to derive a "UV-normalized" dose metric for different test species/endpoints that can then be extrapolated to assess hazards under different UV light exposure scenarios. Criteria that can be used to judge reliability include acceptable control performance, analytically confirmed exposure concentrations and measurement of UV-A light irradiance.

3.3. ANALYSIS FRAMEWORK FOR EXTRAPOLATING LAB RESULTS TO MODEL SCENARIOS

The average irradiances of surface UV-A light during both summer and winter periods at 40°N latitude used in evaluating photodegradation (expressed earlier in millieinsteins $cm^{-2}\ d^{-1}$, Eqn 2) correspond to 5579 and 1797 μW cm^{-2}, respectively. Using the extinction coefficients reported in **Table 6**, the UV light exposures averaged over the default 3 m depth for the different model scenarios are summarized in **Table 10**.

Table 10. Average UV Light exposures for evaluating different PAHs and water bodies

Substance	Season	Water Type	UV Light (μW cm^{-2})
Anthracene	Summer	Oligotrophic	1411
	Winter	Oligotrophic	454
	Summer	Eutrophic	133
	Winter	Eutrophic	43
Fluoranthene	Summer	Oligotrophic	1080
	Winter	Oligotrophic	348
	Summer	Eutrophic	103
	Winter	Eutrophic	33
Pyrene	Summer	Oligotrophic	786
	Winter	Oligotrophic	253
	Summer	Eutrophic	77
	Winter	Eutrophic	25
Benzo(a)pyrene	Summer	Oligotrophic	1509
	Winter	Oligotrophic	486
	Summer	Eutrophic	159
	Winter	Eutrophic	51

To translate toxicity metrics described in the previous section to phototoxicity hazard for the different modelling scenarios a daily duration of UV light exposure must be assumed. **Figure 5** shows that the day length (defined as time between sunset and sunrise) varies as a function of latitude. From this graph a day length of 15 h and 9 h can be assumed for the summer and winter periods at 40°N latitude that correspond to the scenarios considered in this study.

It is now possible to illustrate how UV-normalized lab toxicity metrics can be related to the different modelling scenarios. In the study by Ankley et al. [21], the 20 h LT_{50} for pyrene with the oligochaete, *Lumbriculus variegatus* is estimated to be 1800 μW cm^{-2} mg g_{tissue}^{-1}. The mean bioconcentration factor for pyrene was reported to be 1720 L/kg tissue. Thus, the 24 h UV-normalized toxicity metric can be determined:

1800 µW cm^{-2} mg g_{tissue}^{-1} / (1720 L/kg_{tissue} x 0.001 kg_{tissue}/g_{tissue}) x 20 h /24 h = 872 µW cm^{-2} µg $\boldsymbol{L^{-1}}$.

The $LC_{50,UV}$ for pyrene corresponding to summer in an oligotrophic water body can now be estimated as:

$LC_{50,UV}$ = 872 µW cm^{-2} µg $\boldsymbol{L^{-1}}$ x 24 h / (786 µW cm^{-2} x 15 h) = 1.77 µg/L

For the winter scenario in an eutrophic water body, the estimated $LC_{50,UV}$ can be calculated as:

872 µW cm^{-2} µg $\boldsymbol{L^{-1}}$ x 24 h / (25 µW cm^{-2} x 9 h) = 93.0 µg/L

Figure 5. Day length by month for different latitudes [Used by permission of Alastair Reid (2020)]

Source:http://wordpress.mrreid.org/2014/10/19/rate-of-change-of-day-length-with-latitude/

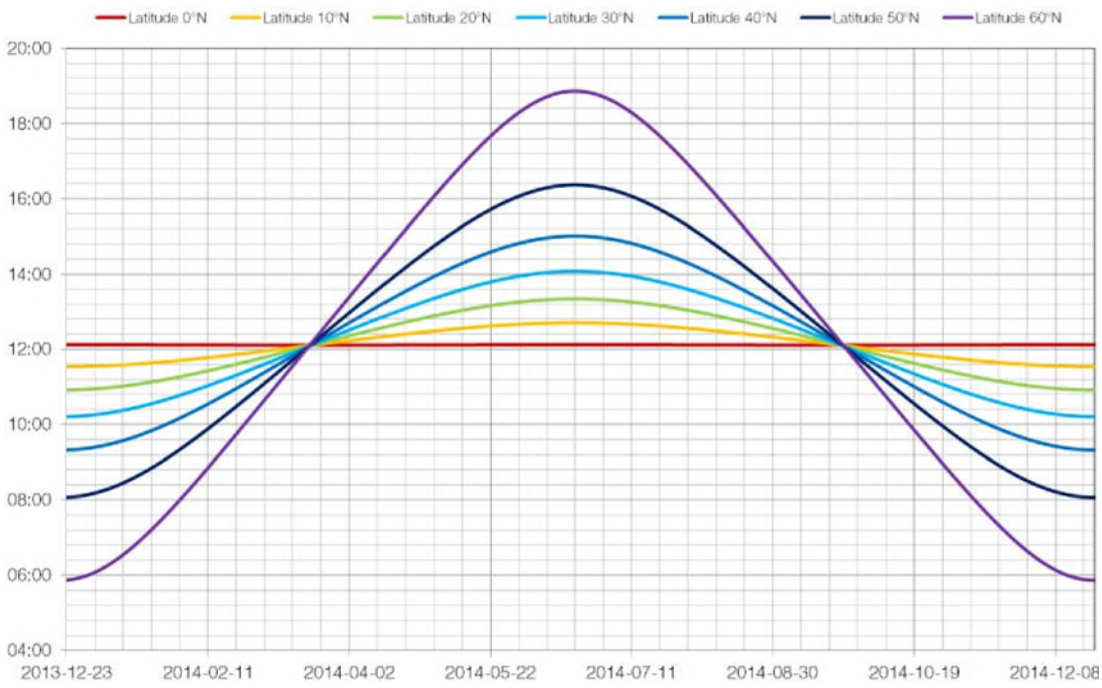

Using the alternative UV light exposure derived from **Table 9**, the estimated algal $EC_{50,UV}$ for anthracene for the summer scenario in an oligotrophic water is:

2778 µW cm^{-2} µg $\boldsymbol{L^{-1}}$ d x 24 h / (1411 µW cm^{-2} x 15 h) = 3.1 µg/L

while for the winter scenario in an oligotrophic water the value increases to:

2778 µW cm^{-2} µg $\boldsymbol{L^{-1}}$ d x 24 h/d / (43 µW cm^{-2} x 9 h) = 172.3 µg/L

This later value exceeds the water solubility of this substance (50 µg/L) suggesting that the phototoxicity hazard posed by this substance under this scenario is of limited concern for this species. This approach is likely conservative since other site-specific factors that can confound extrapolation of lab toxicity data sets to characterize phototoxicity hazard in the field are ignored. For example, lab organisms are typically not acclimated to UV exposures before testing. However, in the field, organisms can adapt or avoid higher UV-light intensities through morphological (i.e. pigmentation) or behavioural adaptations thereby potentially reducing sensitivity to combined chemical-UV light exposures [40].

3.4. PHOTOTOXICITY HAZARD ASSESSMENT FOR REPRESENTATIVE PAHS

Literature data were compiled for each PAH and are summarized in **Tables 11-14**. The tables also specify the UV-light regime used as either continuous (C) or in terms of the experimental light: dark photoperiod. Past work has demonstrated that toxicity results generated under continuous UV exposure are more conservative than toxicity tests that include a dark period allowing damage repair [24]. Thus, dose metrics derived from studies using a continuous UV source are expected to be conservative. Data for freshwater and marine species as well as acute and chronic endpoints have been combined as past work does not indicate clear systematic differences between organisms or endpoints [25]. Fluoranthene has the largest available dataset covering over 20 different test species (**Table 12**). Smaller data sets are available for anthracene and pyrene and indicate more than a two order of magnitude difference in organism sensitivity (**Table 11, 13**). Only limited hazard data are available for benzo(a)pyrene (**Table 14).** Species-sensitivity distributions characterizing the normalized photoxicity dose metric for each PAH are provided in **Figure 6**. While there are fewer data for plants and algae the available data suggest these species (denoted by green symbols) are less sensitive than fish (red) and invertebrates (blue) which span a similar range in sensitivity (**Figure 6**). The empirical distributions appear log-normally distributed and span nearly three orders of magnitude exhibiting a similar slope and range across the four PAHs investigated. The assumption of log-normality was tested using several statistical tests (Shapiro, Lillie, and Andersen-Darling) using the log transformed values of the UV normalized doses (**Tables 11-14**). The p-values for these three tests were all >0.1 indicating that the null hypothesis of log-normality is not rejected. The dataset for benz(a)pyrene was too small (n=4) to apply these tests. However, visual inspection of this distribution indicates a similar pattern as the other PAHs (**Figure 6**).

Table 11. Hazard data characterizing the effect of UV light on anthracene toxicity. UV Light specified as C - continuous, or the light: dark cycle in hours

Test Species	Test Endpoint	UV Light	Dose Metric ($\mu W cm^{-2} \mu g\ L^{-1}$)	Summer Oligo Effect Conc. (µg/L)	Winter Oligo Effect Conc. (µg/L)	Summer Eutro Effect Conc. (µg/L)	Winter Eutro Effect Conc.(µg/L)	Reference
Lepomis macrochirus (bluegill sunfish)	NOEC survival	C	120	0.14	0.70	1.44	7.46	Oris & Geisy 1986 [26]
Daphnia magna (cladoceran)	EC_{10} reproduction	16:8	148	0.17	0.87	1.78	9.22	Holst & Geisy 1989 [27]
Danio rerio (zebrafish)	LC_{50} larvae survival**	16:8	152	0.17	0.89	1.83	9.45	Willis & Oris 2014 [17]
Clupea pallasi (pacific herring)	LC_{50} larvae survival	16:8	210	0.24	1.23	2.52	13.1	Jeffries et al 2014 [28]
Hyalella azteca (amphipod)	LC_{50} survival	C	266	0.30	1.56	3.20	16.5	Hatch & Burton 1999 [29]
Chironomus tentans (midge)	LC_{50} survival	C	285	0.32	1.67	3.43	17.7	Hatch & Burton 2001 [29]
Lumbriculus variegatus (oligochaete)	EC_{50} larvae viability*	C	389	0.44	2.28	4.68	24.2	Weinstein & Polk 2001[22]
Ruditapes decussatus (carpet shell clam)	EC_{50} larval hatching	12:12	397	0.45	2.33	4.77	24.7	Fathallal et al. 2012[30]
Lepomis macrochirus (bluegill sunfish)	LC_{50} survival	C	460	0.52	2.70	5.53	28.6	Oris & Geisy 1986 [26]
Mysidopsis bahia (mysid shrimp)	LC_{50} survival	16:8	953	1.08	5.59	11.5	59.3	Pelletier et al. 1997[31]
Lumbriculus variegatus (oligochaete)	LC_{50} survival	C	1312	1.49	7.70	15.8	81.6	Ankley et al 1997 [21]

Mulinia lateralis (surf clam)	EC_{50} embryo development	16:8	1712	1.94	10.0	20.6	106.5	Pelletier et al. 1997[31]
Selenastrum capricornutum (green alga)	EC_{50} growth	C	2778	3.15	16.3	33.4	172.8	Gala & Geisy 1992 [23]
Artemia salina (brine shrimp)	LC_{50} survival	C	3025	3.43	17.8	36.4	188.1	Diamond et al. 2000[32]
Ruditapes decussatus (carpet shell clam)	EC_{10} larval hatching	12:12	4113	4.66	24.1	49.4	255.8	Fathallal et al. 2012[30]
Phaeodactylum tricornutum (diatom)	EC_{50} growth	C	4800	5.4	28.2	57.7	298.5	Wang et al. 2008 [33]
Scenedesmus vacuolatus (green alga)	EC_{10} growth	C	8768	9.94	51.5	105.4	545.3	Grote et al. 2005 [19]
Mulinia lateralis (surf clam)	LC_{50} survival	16:8	18236	20.7	107.0	219.2	1134	Pelletier et al. 1997[31]
	HC_5		144	0.16	0.85	1.73	8.96	

Table 12. Hazard data characterizing the effect of UV light on fluoranthene toxicity

Test Species	Test Endpoint	UV Light	Dose Metric ($\mu W cm^{-2} \mu g\ L^{-1}$)	Summer Oligo Effect Conc. (µg/L)	Winter Oligo Effect Conc. (µg/L)	Summer Eutro Effect Conc. (µg/L)	Winter Eutro Effect Conc (µg/L)	Reference
Pleuronectes americanus (winter flounder)	LC_{50} survival	16:8	40	0.06	0.30	0.61	3.18	Spehar et al 1999 [25]
Clupea pallasi (pacific herring)	LC_{50} embryo survival	17:7	96	0.14	0.74	1.49	7.73	Diamond et al. 2006[32]
Hyalella azteca (amphipod)	LC_{50} survival	16:8	151	0.22	1.16	2.35	12.14	Wilcoxen et al 2003[34]
Lumbriculus variegatus (oligochaete)	EC_{50} larvae viability*	C	159	0.24	1.22	2.47	12.80	Weinstein 2001[35]
Mulinia lateralis (surf clam)	EC_{50} embryo development	16:8	288	0.43	2.21	4.47	23.15	Pelletier et al. 1997 [31]
Hyalella azteca (amphipod)	LC_{50} survival	C	347	0.51	2.66	5.38	27.83	Hatch & Burton 1999 [29]
Mulinia lateralis (surf clam)	LC_{50} survival	16:8	476	0.71	3.65	7.39	38.23	Pelletier et al. 1997 [31]
Lumbriculus variegatus (oligochaete)	LC_{50} survival	12:12	490	0.73	3.75	7.60	39.32	Spehar et al 1999 [25]
Clupea pallasi (pacific herring)	LC_{50} larvae survival	16:8	547	0.81	4.19	8.48	43.87	Jeffries et al 2014 [28]
Mysidopsis bahia (mysid shrimp)	LC_{50} survival	16:8	555	0.82	4.25	8.61	44.53	Spehar et al 1999 [25]
Ruditapes decussatus (carpet shell clam)	EC_{50} larval hatching	12:12	588	0.87	4.50	9.11	47.15	Fathallal et al. 2012 [30]

Chironomus tentans (midge)	LC_{50} survival	C	599	0.89	4.59	9.28	48.03	Hatch & Burton 1999 [29]
Daphnia magna (cladoceran)	LC_{50} survival	12:12	653	0.97	5.01	10.13	52.42	Spehar et al 1999 [25]
Monopylephorus rubroniveus (oligochaete)	LC_{50} survival	C	685	1.02	5.25	10.63	55.01	Weinstein 2003 [36]
Hydra americana (hydra)	LC_{50} survival	12:12	898	1.33	6.88	13.93	72.08	Spehar et al 1999 [25]
Palaemonetes pugio (grass shrimp)	LC_{50} survival	C	901	1.33	6.90	13.97	72.31	Weinstein 2003 [36]
Mulinia lateralis (surf clam)	LC_{50} embryo larval survival	16:8	1110	1.64	8.50	17.21	89.06	Spehar et al 1999 [25]
Artemia salina (brine shrimp)	LC_{50} immobilization	C	1237.5	1.83	9.48	19.19	99.32	Diamond et al. 2000 [32]
Mysidopsis bahia (mysid shrimp)	LC_{50} survival	16:8	1408	2.09	10.79	21.84	113.0	Pelletier et al. 1997 [31]
Arbacia punctulata (sea urchin)	LC_{50} survival	16:8	1546	2.29	11.84	23.97	124.0	Spehar et al 1999 [25]
Pimephales promelas (fathead minnow)	LC_{50} juvenile survival	C	1578	2.34	12.09	24.48	126.7	Weinstein & Oris 1999 [37]
Lumbriculus variegatus (oligochaete)	LC_{50} survival	C	2248	3.33	17.23	34.87	180.4	Ankley et al 1997 [21]
Daphnia magna (cladoceran)	NOEC growth	12:12	2406	3.56	18.43	37.31	193.1	Spehar et al 1999 [25]
Macoma liliana (wedge shell clam)	EC_{50} ability to bury	1:23	2492	3.69	19.09	38.65	200.0	Ahrens et al. 2002 [41]
Ruditapes decussatus (carpet shell clam)	EC_{10} larval hatching	12:12	2656	3.93	20.35	41.20	213.2	Fathallal et al.2012[30]
Oncorhynchus mykiss (rainbow trout)	LC_{50} survival	12:12	3144	4.66	24.09	48.76	252.3	Spehar et al 1999 [25]

Pimephales promelas (fathead minnow)	NOEC growth	12:12	3182	4.71	24.38	49.36	255.4	Spehar et al 1999 [25]
Scenedesmus vacuolatus (green alga)	EC_{10} growth	C	3222	4.77	24.69	49.97	258.6	Grote et al. 2005 [19]
Mysidopsis bahia (mysid shrimp)	NOEC reproduction	16:8	4399	6.51	33.71	68.23	353.1	Spehar et al 1999 [25]
Pimephales promelas (fathead minnow)	LC_{50} survival	12:12	4981	7.38	38.16	77.25	399.7	Spehar et al 1999 [25]
Lepomis macrochirus (bluegill sunfish)	LC_{50} juvenile survival	12:12	5021	7.44	38.48	77.88	403.0	Spehar et al 1999 [25]
Homarus americanus (american lobster)	LC_{50} survival	5152	7.63	39.48	39.48	79.91	413.5	Spehar et al 1999 [25]
Phaeodactylum tricornutum (diatom)	EC_{50} growth	C	7200	10.66	55.17	111.7	577.8	Wang et al. 2008 [33]
Rana pipens (leopard frog)	LC_{50} larvae survival	C	8182	12.12	62.69	126.9	656.6	Monson et al 1999 [38]
Palaemonetes species (grass shrimp)	LC_{50} survival	16:8	8719	12.91	66.81	135.2	699.8	Spehar et al 1999 [25]
Menidia beryllina (Inland silverside)	LC_{50} survival	16:8	11890	17.61	91.11	184.4	954.2	Spehar et al 1999 [25]
Physella virgata (snail)	LC_{50} survival	12:12	19393	28.72	148.6	300.8	1556	Spehar et al 1999 [25]
Ophiogomphus species (dragonfly)	LC_{50} nymph survival	12:12	26015	38.52	199.3	403.5	2088	Spehar et al 1999 [25]
Lemna minor (duckweed)	LC_{50} growth	12:12	37604	55.68	288.1	583.2	3018	Spehar et al 1999 [25]
Cyprinodon variegatus (sheepshead minnow)	LC_{50} survival	16:8	63017	93.32	482.9	977.4	5057	Spehar et al 1999 [25]
	HC_5		149	0.22	1.14	2.31	11.96	

Table 13. Hazard data characterizing the effect of UV light on pyrene toxicity

Test Species	Test Endpoint	UV Light	Dose Metric ($\mu W cm^{-2} \mu g\ L^{-1}$)	Summer Oligo Effect Conc. (µg/L)	Winter Oligo Effect Conc. (µg/L)	Summer Eutro Effect Conc. (µg/L)	Winter Eutro Effect Conc (µg/L)	Reference
Ceriodaphnia dubia (cladoceran)	EC_{10} reproduction	16:8	57	0.12	0.60	1.18	6.09	Butler et al 2014 [39]
Mulinia lateralis (surf clam)	EC_{50} embryo development	16.8	61	0.12	0.64	1.26	6.52	Pelletier et al.1997 [31]
Utterbackia imbecillis (paper pondshell)	EC_{50} larvae viability*	C	201	0.41	2.12	4.17	21.6	Weinstein & Polk 2001 [22]
Mysidopsis bahia (mysid shrimp)	LC_{50} survival	16.8	236	0.48	2.48	4.88	25.2	Pelletier et al. 1997 [31]
Danio rerio(zebrafish)	LC_{50} larvae survival**	16:8	247	0.50	2.60	5.11	26.4	Willis & Oris 2014 [17]
Clupea pallasi (pacific herring)	LC_{50} *larvae survival*	16:8	251	0.51	2.64	5.19	26.9	Jeffries et al 2014 [28]
Ruditapes decussatus (carpet shell clam)	EC_{50} *larval hatching*	12:12	306	0.62	3.23	6.34	32.8	Fathallal et al. 2012 [30]
Mulinia lateralis (surf clam)	LC_{50} *survival*	16:8	445	0.91	4.68	9.21	47.6	Pelletier et al. 1997 [31]
Danio rerio (zebrafish)	LC_{50} *embryo survival*	12:12	475	0.97	5.00	9.83	50.9	Butler et al 2014 [39]
Artemia salina (brine shrimp)	LC_{50} *survival*	C	845	1.72	8.90	17.5	90.5	Diamond et al. 2000 [32]
Lumbriculus variegatus (oligochaete)	LC_{50} *survival*	C	872	1.78	9.19	18.1	93.5	Ankley et al 1997 [21]
Ruditapes decussatus (carpet shell clam	EC_{10} *larval hatching*	12:12	1258	2.56	13.2	26.0	134.8	Fathallal et al. 2012 [30]

Benthic Algae (mostly diatoms)	*LOEC Photosynthesis*	4:20	3097	6.31	32.6	64.1	331.9	Petersen et al. 2008 [42]
Scenedesmus vacuolatus (green alga)	*EC_{10} growth*	C	3256	6.63	34.3	67.4	348.9	Grote et al. 2005 [19]
Phaeodactylum tricornutum (diatom)	*EC_{50} growth*	C	9120	18.6	96.1	188.9	977.3	Wang et al. 2008 [33]
	HC_5		60	0.12	0.63	1.24	6.43	

Table 14. Hazard data characterizing the effect of UV light on benzo(a)pyrene to toxicity

Test Species	Test Endpoint	UV Light	Dose Metric (µW cm^{-2} µg L^{-1})	Summer Oligo Effect Conc. (µg/L)	Winter Oligo Effect Conc. (µg/L)	Summer Eutro Effect Conc. (µg/L)	Winter Eutro Effect Conc (µg/L)	Reference
Ruditapes decussatus (carpet shell clam)	*EC_{50}* larval hatching	12:12	58	0.06	0.32	0.58	3.02	Fathallal et al. 2012[30]
Ruditapes decussatus (carpet shell clam)	*EC_{10}* larval hatching	12:12	257	0.27	1.41	2.58	13.37	Fathallal et al. 2012[30]
Scenedesmus vacuolatus (green alga)	*EC_{10}* growth	C	263	0.28	1.44	2.65	13.71	Grote et al. 2005 [19]
Clupea pallasi (pacific herring)	*LC_{50}* larvae survival	16:8	2935	3.11	16.10	29.56	153.0	Jeffries et al 2014 [28]
	HC_5		88	0.09	0.48	0.89	4.59	

Figure 6. Distribution of UV-normalized toxicity data for representative PAHs

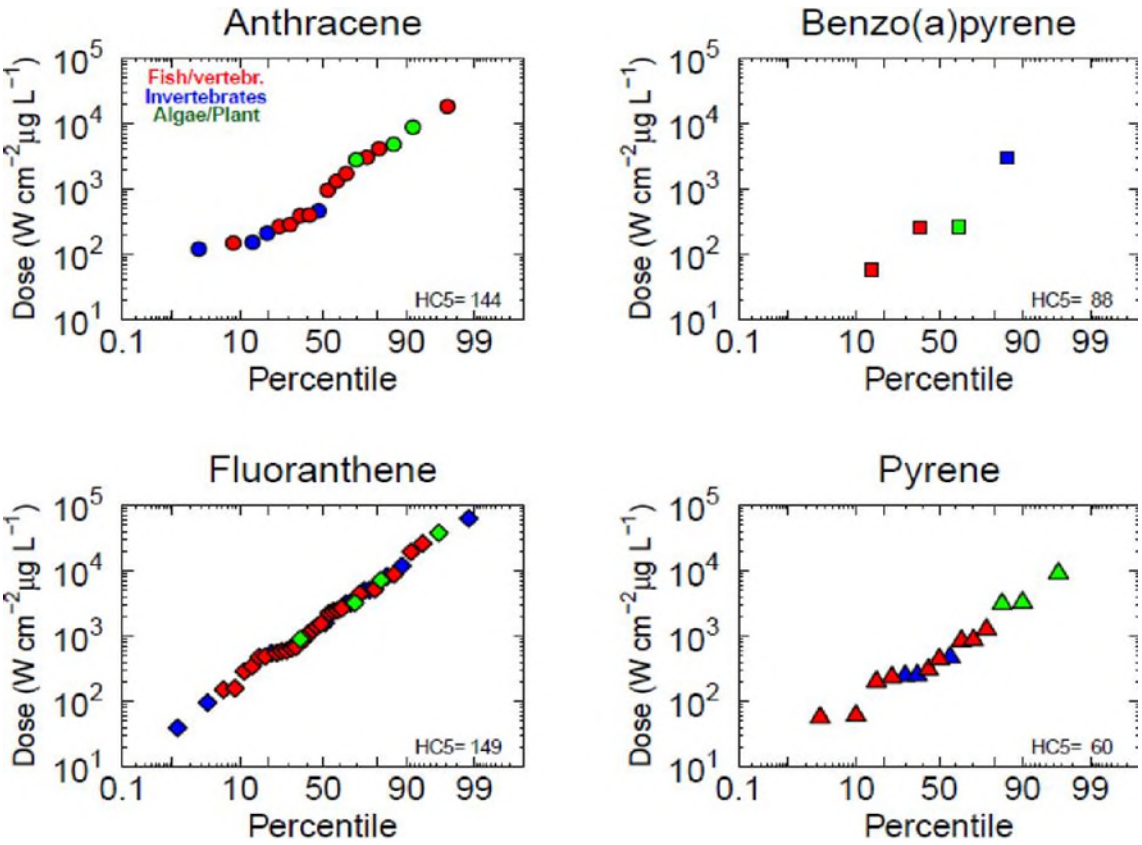

The 5th percentile of the log-normalized UV-normalized doses was computed for each PAH and found to fall within a narrow range from 60 µW $\boldsymbol{cm^{-2}}$ µg $\boldsymbol{L^{-1}}$ for pyrene to 149 µW $\boldsymbol{cm^{-2}}$ µg $\boldsymbol{L^{-1}}$ for fluoranthene. These values were then used to compute HC_5 values corresponding to the different seasons and water bodies based on the UV light intensities from Table 10 and assumed day lengths (15 h summer; 9 h winter) (**Tables 11-14**). Predicted effect concentrations for a given species/ endpoint varies by about a factor of 50 between the different scenarios. These values are compared to HC_5 values derived using the updated target lipid model (TLM) [43] which are intended to protect aquatic life from chronic exposures without consideration of the potential modulating effects of UV-light exposures (**Table 15**). Results indicate that for the summer scenario in an oligotrophic water body that provides a high degree of UV light penetration the $HC_{5,UV}$ for anthracene is almost 30-fold lower than the HC_5 derived using the TLM. For the other PAHs, the $HC_{5,UV}$ is <2 to 12.5 fold lower for this worst case scenario with benzo(a)pyrene exhibiting the lowest ratio (i.e. exhibiting the least enhancement in toxicity). For the other exposure scenarios, discrepancies between the HC_5 values are less pronounced.

Table 15. Comparison of HC_5 values derived with and without consideration of UV light exposures

Substance	Summer Oligo	Winter Oligo	Summer Eutro	Winter Eutro
Anthracene				
$HC_{5,UV}$ (µg/L)	0.16	0.85	1.73	8.96
$HC_{5,TLM}$ (µg/L)	4.7	4.7	4.7	4.7
Ratio	0.03	0.18	0.37	1.91
Fluoranthene				
$HC_{5,UV}$ (µg/L)	0.22	1.14	2.31	11.96
$HC_{5,TLM}$ (µg/L)	1.5	1.5	1.5	1.5
Ratio	0.15	0.76	1.54	7.97
Pyrene				
$HC_{5,UV}$ (µg/L)	0.12	0.63	1.24	6.43
$HC_{5,TLM}$ (µg/L)	1.5	1.5	1.5	1.5
Ratio	0.08	0.42	0.83	4.29
Benzo(a)pyrene				
$HC_{5,UV}$ (µg/L)	0.09	0.48	0.89	4.59*
$HC_{5,TLM}$,(µg/L)	0.14	0.14	0.14	0.14
Ratio	0.64	3.43	6.357	>11.43

*This value exceeds the water solubility of this test substance; to compute a lower bound HC_5 ratio a water solubility of 1.6 µg/L has been assumed

3.5. IMPLICATIONS FOR RISK CHARACTERIZATION

The previous sections have quantified the mitigating role that sunlight plays in reducing exposure as a result of photodegradation while increasing hazard as a result of photoenhanced toxicity. The objective of this section is to discuss the implications of these combined processes on risk characterization in the aquatic compartment. Risk quotients (RQ) are defined as the ratio of the PEC to a predicted no-effect concentration (PNEC).

$$RQ = PEC \ / \ PNEC \quad (9)$$

The HC_5 values presented in table 15 are used to represent the PNEC.The PECs presented in this analysis (**Table 8**) represent differences in predicted substance exposures between scenarios since the same tonnage was used. The relative impact of UV interactions on RQs was evaluated by first comparing the ratio of the TLM-derived HC_5 (HC_{5tlm}) to the UV-based hazard values derived above (HC_{5UV}). The ratios of hazard values range from less than 1 (e.g., $HC_{5tlm} > HC_{5UV}$) to 30-fold (**Table 15**). For comparison the ratio of PECs with and without UV-induced photodegradation range from approximately 1 (e.g., $PEC_{photo} = PEC_{biodeg}$) to 100-fold (**Table 8**). A key finding is that the relative changes in hazard and exposure are of the same order of magnitude.

Specific comparisons of the PEC ratios calculated from **Table 8** to the HC_5 ratios reported Table in 15 shows that the relative changes in the RQs vary from a factor of 0.01 to 2 (**Table 16**). The RQ ratios less than one indicate photodegradation is the major process, outcompeting phototoxicity, while ratios greater than one indicate that phototoxicity is more important. The lowest ratio is 0.01 for benzo(a)pyrene B(a)P for the oligotrophic, summer scenario, and the highest ratio is ca. 2 for fluoranthene for the same scenario. B(a)P has relatively fast photodegradation rates across the scenarios relative to other losses processes coupled with a relatively low photo-induced toxicity potential when contrasted to the TLM-derived chronic effects concentration (**Table 15**).

Table 16. Comparison of RQ Ratios with and without consideration of UV light

Substance	Summer Oligo	Winter Oligo	Summer Eutro	Winter Eutro
Anthracene				
PEC_{UV}/PEC_{no-UV}	0.02	0.06	0.18	0.42
$HC_{5,UV}/HC_{5,TLM}$	0.03	0.18	0.37	1.91
Ratio of RQs	0.66	0.36	0.48	0.22
Fluoranthene				
PEC_{UV}/PEC_{no-UV}	0.31	0.57	0.83	0.94
$HC_{5,UV}/HC_{5,TLM}$	0.15	0.76	1.54	7.97
Ratio of RQs	2.08	0.75	0.54	0.12
Pyrene				
PEC_{UV}/PEC_{no-UV}	0.06	0.17	0.41	0.68
$HC_{5,UV}/HC_{5,TLM}$	0.08	0.42	0.83	4.29
Ratio of RQs	0.79	0.40	0.50	0.16
Benzo(a)pyrene				
PEC_{UV}/PEC_{no-UV}	0.01	0.04	0.14	0.35
$HC_{5,UV}/HC_{5,TLM}$	0.64	3.43	6.36	11.43
Ratio of RQs	0.02	0.01	0.02	0.03

In contrast, fluoranthene has the slowest photodegradation rate of the four PAHs, which results in relatively higher exposure concentrations that exert phototoxicity. This latter case is the only scenario where the risk associated with photoxicity is not more than offset by reductions in predicted exposures as a result of photodegradation processes. Thus, only one of the 16 scenarios investigated indicated the potential for a two-fold higher risk in the presence of UV exposures than when UV exposures were ignored.

There are nine petroleum substance categories that include measureable levels of 3+ring PAHs, mainly gas oils, heavy fuel oils, and residual aromatic extracts (**Table 17**). The other categories are too light (e.g., kerosene, naphtha) or they contain refined substances without aromatics (e.g. waxes mineral oils). The mass abundance of the 3+ ring PAHs in these substances range from 0.45% to 7.3% (C_{12}-C_{20} PAH) with heavy fuel oil and cracked gas oils containing typically higher amounts. The 3+ring PAHs are generally strong contributors to the overall RQs (>10%) to these categories. If the RQ from the 3+ring PAHs were increased by 2-fold, consistent with the highest increase in fluoranthene (**Table 17**), then it follows that the total RQphoto would increase by no more than 2-fold. However, not all of the 3+ ring PAHs are photoactive, and the increase in RQPAH by 2-fold does not apply to those PAH that are not photoactive. Therefore, this analysis indicates that inclusion of UV light interactions in the risk assessment framework will not substantially increase risk characterization ratios. However, since photodegradation processes appear to reduce exposures to a broader range of PAHs than UV light enhances toxicity, RQs for petroleum substances may in fact be reduced when compared to the no-UV light model framework implemented for REACH dossiers (i.e. RQs derived using PETRORISK are conservative when applied to PAH containing petroleum substances).

Table 17. Average Amount of 3+ Ring PAHs in Major Petroleum Substance Categories.

Category	Mass % PAH in substance [a]
Heavy Fuel Oils	6.9
Vacuum Gas Oils	1.3
Cracked Gas Oils	7.3
Straight Run Gas Oils	2.6
Other Gas Oils	0.79
Untreated Aromatic Oils	2.8
Distillate Aromatic Extracts	3
Treated Distillate Aromatic Extracts	0.62
Residual Aromatic Extracts	0.45

[a] Sum of C_{12}-C_{20} PAH blocks which include anthracene, fluoranthene, pyrene, and benzo(a)pyrene

As noted earlier in his report, the role of UV light is expected to vary spatially and temporally. Several studies using passive sampling devices and mussel tissue as monitoring tools have shown a decrease in PAH concentrations in water during summer compared to concentrations in other seasons in locations like the Baltic Sea, the Danube and the coast of South Africa [44, 45, 46]. This decrease has been attributed to seasonal variations in PAH deposition and water temperature. However, changes in photodegradation rates, which were not considered in these studies, could also contribute to the seasonal variation in PAH concentrations.

Thus the absolute importance of UV light on substance hazard and exposure assessment will be variable and site-specific. However, this analysis suggests that incorporation of UV light into risk evaluation impacts both hazard and exposure assessment to comparable degrees and as a result does not significantly increase estimated risks to the aquatic environment. Further, since inclusion of photodegradation in multimedia models reduces human exposure to PAHs [47], neglecting this process provides conservative estimates of health risk.

4. GLOSSARY

B(a)P	Benzo(a)pyrene
BioHCwin	Estimation program software that estimates biodegradation half-life for compounds containing only carbon and hydrogen (i.e. hydrocarbons).
DOC	Dissolved Organic Carbon
EC_{10}	The concentration of a substance at which it is calculated that 10% of the animals will be affected, based on the observed results in a study.
EC_{50}	The concentration of a substance at which it is calculated that 50% of the animals will be affected, based on the observed results in a study
eV	Electron Volts
EUSES	European Union System for the Evaluation of Substances
HC	Hazardous Concentration
HLG	Homo-lumo Gap
K_o	Photodegradation rate constant in "clean" water
LC_{50}	The lethal concentration of a substance at which 50% of the organisms exposed to that substance are killed
NOEC	No Observed Effect Concentration; The concentration of a substance below which no effects to an exposed organism were observed in a study
PAHs	Polyaromatic Hydrocarbons
PECs	Predicted Environmental Concentrations
PNEC	Predicted No-effect Concentration
PETRORISK	Concawe's modelling tool to assess exposure of petroleum substances
REACH	Registration, Evaluation, Authorization and Restriction of Chemicals is a European Union regulation
RQ	Risk Quotients
STP	Sewage Treatment Plant
TLM	Target Lipid Model is a QSAR model that relates chemical structure to toxicity using critical target lipid body burdens for chemicals with a narcotic mode of action
USEPA	United States Environmental Protection Agency
UV	Ultraviolet (UV) is a form of electromagnetic radiation with wavelength from 10 nm to 400 nm (750 THz)

5. REFERENCES

1. Redman, A.D., Parkerton T.F, Comber M.H.I, Leon Paumen, M., Eadsforth C.V, Dmytrasz, B., King, D., Warren, CS., den Haan, KH, Djemel, N. (2014) PETRORISK: a risk assessment framework for petroleum substances. *Integr. Environ. Assess. Manag*. 10, 437–448

2. CONCAWE (2013) Challenges in addressing phototoxicity and photodegradation in the environmental risk assessment of Polycyclic Aromatic Hydrocarbons in the aquatic compartment. Report No. 09/13. Brussels: CONCAWE

3. Mill, T. (2000) Photoreactions in Surface Waters. In: Handbook of Property Estimation Methods for Chemicals, edited by R.S Boethling and D. Mackay, Lewis Publ, Boca Raton, Florida, p. 355-381

4. Chapra, S.C. (1997) Surface Water-Quality Modeling. McGraw-Hill, New York, N.Y. p. 844

5. Schwarzenbach, R. P., Gschwend, P. M., Imboden, D. M. (2005) Environmental Organic Chemistry. John Wiley & Sons, Inc., Hoboken, NJ, USA.

6. USEPA (1998) Fate, Transport and Transformation Test Guidelines OPPTS 835.2210: Direct Photolysis Rate in Water by Sunlight. Prevention, Pesticides and Toxic Substances, United States Environmental Protection Agency, EPA 712-C-98-060, Washington, DC 35pp

7. Fasnacht, M.P., Blough, N.V. (2002) Aqueous Photodegradation of Polycyclic Aromatic Hydrocarbons, *Environ. Sci. Technol. 36, 4364-4369*

8. Mills, W.B, Porcella D.B, Ungs, M.J, Gherini, S.A, Summers, K.V, Mok, L., Rupp, G.L., Bowie, G.L, Haith, D.A. (1985) A Screening Procedure for Toxic and Conventional Pollutants in Surface and Ground Water—Part I (Revised-1985), United States Environmental Protection Agency, Environmental Research Laboratory, Athens GA USA, EPA report 600/6-85/002a, p.444 + 10 appendices

9. Xia, X., Li, G., Yang, Z., Chen, Y., Huang G.H. (2009) Effects of fulvic acid concentration and origin on photodegradation of polycyclic aromatic hydrocarbons in aqueous solution: Importance of active oxygen, *Environmental Pollution, 157, 1352-1359*

10. Clark, C.D, De Bruyn, W.J., Ting, J., Scholle, W. (2007) Solution medium effects on the photochemical degradation of pyrene in water, *Journal of Photochemistry and Photobiology A: Chemistry 186, 342-348*

11. Jacobs, L.E, Weavers, L.K, Chin, Y-P (2008) Direct and indirect photolysis of polycyclic aromatic hydrocarbons in nitrate-rich surface waters. *Environ. Toxicol. Chem., 27, 1643-1648*

12. de Bruyn, W.J, Clark, C.D, Ottelle, K., Aiona, A. (2012) Photochemical degradation of phenanthrene as a function of natural water variables modeling freshwater to marine environments. *Marine Pollution Bulletin 64,532-538*

13. Castro-Jiminez, J., van de Meent, D. (2011) Accounting for Photodegradation in the PBT Assessment of Chemicals, Reports Environmental Science no 381, Radboud University Nijmegen, Nijmegen, The Nethelands, 53 pp

14. Howard, P., Meylan, W., Aronson, D., Stiteler, W., Tunkel, J., Comber, M., Parkerton, T.F (2005) A New Biodegradation Prediction Model Specific to Petroleum Hydrocarbons. *Environ.Toxicol. and Chem. Vol. 24(8), 1847-1860*

15. Kot-Wasik, A., Dabrowska, D., Namieśnik, J. (2004) Photodegradation and biodegradation study of benzo(a)pyrene in different liquid media. *Journal of Photochemistry and Photobiology A: Chemistry 168, 109-115*

16. Geisy, J.P, Newsted, J.L, Oris, J.T. (2013) Photo-Enhanced Toxicity: Serendipity of a Prepared Mind and Flexible Program Management. *Environ. Toxicol. Chem. 32, 969-971*

17. Willis, A.M., Oris J.T. (2014) Acute photo-induced toxicity and toxicokinetics of single compounds and mixtures of polycyclic aromatic hydrocarbons in zebrafish. *Environ. Toxicol. Chem. 33, 2028-2037*

18. Mekenyan, O.G., Ankley, G.T., Veith, G.D, Call, D.J. (1994) QSARs for photoinduced toxicity: I. Acute lethality of polycyclic aromatic hydrocarbons to *Daphnia magna*. *Chemosphere 28, 567-582*

19. Grote, M., Schuurmann, G., Altenburger, R. (2005) Modeling Photoinduced Algal Toxicity of Polycyclic Aromatic Hydrocarbons. *Environ. Sci. Technol. 39, 4141-4149*

20. Veith, G.D, Mekenyan, O.G, Ankley, G.T, Call, D.J. (1995) A QSAR analysis of substituent effects on the photoinduced toxicity of PAHs. *Chemosphere 30, 2129-2142*

21. Ankley, G. T., Erickson, R. J., Sheedy, B. R., Kosian, P. A., Mattson, V. R., Cox, J. S. (1997) Evaluation of models for predicting the phototoxic potency of polycyclic aromatic hydrocarbons. *Aquat. Toxicol. 37, 37-50*

22. Weinstein, J.E, Polk, K.D. (2001) Phototoxicity of anthracene and pyrene to glochidia of the freshwater mussel U*tterbackia imbecillis. Environmental Toxicology and Chemistry 20, 2021-2028*

23. Gala, W.R., Giesy, J.P. (1992) Photo-induced toxicity of anthracene to the green algae, Selenastrum capricornutum. *Arch. Environ. Contam. Toxicol. 23, 316-323*

24. Weinstein, J.E., Diamond, S.A. (2006) Relating daily solar UV radiationdose in salt marsh-associated estuarine systems to laboratory assessments of photoactivated PAH toxicity. *Environ. Toxicol. Chem. 25(11), 2860-2868*

25. Spehar, R.L., Poucher, S., Brooke, L.T., Hansen, D.J., Champlin, D., Cox, D.A. (1999) Comparative toxicity of fluoranthene to freshwater and saltwater species under fluorescent and ultraviolet light. *Arch. Environ. Contam. Toxicol. 37, 496-502*

26. Oris, J.T., Giesy, J.P. (1986) Photoinduced toxicity of anthracene to juvenile bluegill sunfish (*Lepomis macrochirus* Rafinesque): Photoperiod effects and predictive hazard evaluation. *Environ. Toxicol. Chem. 5, 761-768*

27. Holst, L.L., Giesy, J.P. (1989) Chronic effects of the photoenhanced toxicity of anthracene on Daphnia magna reproduction. *Environ. Toxicol. Chem. 8, 933-942*

28. Jeffries, M.K.S., Claytor, C., Stubblefield, W., Pearson, W.H., Oris, J.T. (2013) Quantitative risk model for polycyclic aromatic hydrocarbon photoinduced toxicity in Pacific herring following the Exxon Valdez oil spill. *Environ. Sci. Technol. 47, 5450-5458*

29. Hatch, A.C., Burton Jr., G.A. (1999) Photo-induced toxicity of PAHs to Hyalella Azteca and Chironomus tentans: Effects of mixtures and behaviour. *Environ. Pollut. 106,157-167*

30. Fathallah, S., Medhioub, M.N, Kraiem, M.M. (2012) Photo-induced Toxicity of Four Polycyclic Aromatic Hydrocarbons (PAHs) to Embryos and Larvae of the Carpet ShellClam Ruditapes decussatus. *Bull. Environ. Contam. Toxicol. 88, 1001-1008*

31. Pelletier, M.C., Burgess, R.M, Ho, K.T, Kuhn, A., McKinney R.A, Ryba, S.A. (1997) Phototoxicity of individual polycyclic aromatic hydrocarbons and petroleum to marine invertebrate larvae and juveniles. *Environ. Toxicol. Chem. 16, 2190-2199*

32. Diamond, S.A., Mount, D.R., Burkhard, L.P., Ankley, G.T., Makynen E.A., Leonard, E.N. (2000) Effect of irradiance spectra on the photoinduced toxicity of three polycyclic aromatic hydrocarbons. *Environ. Toxicol. Chem. 19, 1389-1396*

33. Wang, L., Zheng, B., Meng, W. (2008) Photo-induced toxicity of four polycyclic aromatic hydrocarbons, singly and in combination, to the marine diatom Phaeodactylum tricornutum. *Ecotoxicol. Environ. Saf. 71, 465-472*

34. Wilcoxen, S.E., Meier, P.G., Landrum, P.F. (2003) The toxicity of fluoranthene to Hyalella azteca in sediment and water-only exposures under varying light. *Ecotoxicol. Environ. Saf. 54, 105-117*

35. Weinstein J.E. (2001) Characterization of the acute toxicity of photoactivated fluoranthene to glochidia of the freshwater mussel, Utterbackia imbecillis. *Environ. Toxicol. Chem. 20, 412-419*

36. Weinstein, J.E. (2003) Influence of salinity on the bioaccumulation and photoinduced toxicity of fluoranthene to an estuarine shrimp and oligochaete. *Environ. Toxicol. Chem.22, 2932-2939*

37. Weinstein, J.E. (1999) Humic acids reduce the bioaccumulation and photoinduced toxicity of fluoranthene to fish. *Environ. Toxicol. Chem.18, 2087-2094*

38. Monson, P.D., Call, D.J., Cox, D.A, Liber, K., Ankley, G.T. (1999) Photoinduced toxicity of fluoranthene to northern leopard frogs (Rana pipiens). *Environ. Toxicol. Chem. 18, 308-312*

39. Butler J., et al. (2015) Phototoxicity of PAH to Ceriodaphnia dubia. SETAC-Europe 2015 Barcelona, ES

40. McDonald, B.G., Chapman, P.M. (2002) PAH phototoxicity – an ecologically irrelevant phenomenon. *Marin. Pollut. Bull. 44, 1321-1326*

41. Ahrens, M.J., Nieuwenhuis, R., Hickey, C.W. (2002) Sensitivity of Juvenile Macomona liliana (bivalvia) to UV-Photoactivated Fluoranthene Toxicity. *Environ. Toxicol. 17, 567–577*

42. Petersen, D.G., Reichenberg, F., Dahloff, I. (2008) Phototoxicity of Pyrene Affects Benthic Algae and Bacteria from the Arctic. *Environ. Sci. Techol. 42, 1371-1376*

43. HDR (2015) Refinement and Validation of TLM-Derived HC5 Values, Report to CONCAWE, Brussels, Belgium, 70 pp + Appendices

44. Amdany, R., Chimuka, L., Cukrowska, E., Kukučka, P., Kohoutek, J., Vrana, B. Investigating the temporal trends in PAH, PCB and OCP concentrations in Hartbeespoort Dam, South Africa, using semipermeable membrane devices (SPMDs). The South African Water Commission, 40(3)

45. Vrana, B., Klučárovác, V., Benickác, E., Abou-Mradb, N., Amdanyd, R., Horákováa, S., Draxlere, A., Humere, F., Ganse, O. Passive sampling: An effective method for monitoring seasonal and spatial variability of dissolved hydrophobic organic contaminants and metals in the Danube River. *Environ. Poll. 184,101-112*

46. Olenycza, M., Sokolowskia, A., Niewińskaa, A., Wolowicza, M., Namieśnikb, J., Hummelc, H., Jansen, J. (2015) Comparison of PCBs and PAHs levels in European coastal waters using mussels from the Mytilus edulis complex as biomonitors. *Oceanologia 57, 196-211*

47. Li, D., Huijbregts, M.A.J, Jolliet, O. (2015). Life cycle health impacts of polycyclic aromatic hydrocarbon for source-specific mixtures. *Int. J. Life Cycle Assess.* 20, 87–99

APPENDIX

PAH concentration =		0.000396354	moles/L					
	Wavelength				λ center		Summer	Winter
Interval	nm	A	ε_λ		(nm)	ε_λ	L_λ	L_λ
1	297.5	3.20	8074		297.5	8074	6.17E-05	5.49E-07
2	300.0	3.10	7821		300	7821	2.70E-04	5.13E-06
3	302.5	3.00	7569		302.5	7569	8.30E-04	3.02E-05
4	305.0	2.50	6308		305	6308	1.95E-03	1.19E-04
5	307.5	1.80	4541		307.5	4541	3.74E-03	3.38E-04
6	310.0	1.20	3028		310	3028	6.17E-03	7.53E-04
7	312.5	0.90	2271		312.5	2271	9.07E-03	1.39E-03
8	315.0	0.90	2271		315	2271	1.22E-02	2.22E-03
9	317.5	0.80	2018		317.5	2018	1.55E-02	3.19E-03
10	320.0	0.70	1766		320	1766	1.87E-02	4.23E-03
11	322.5	0.70	1766		323.1	1766	3.35E-02	8.25E-03
12	325.0	0.80	2018		330	2927	1.10E-01	3.16E-02
13	327.5	1.00	2523		340	4138	1.46E-01	4.31E-02
14	330.0	1.20	3028		350	6408	1.62E-01	4.98E-02
15	332.5	1.40	3532		360	6863	1.79E-01	5.68E-02
16	335.0	1.40	3532		370	6762	1.91E-01	6.22E-02
17	337.5	1.30	3280		380	6812	2.04E-01	6.78E-02
18	340.0	1.40	3532		390	5551	1.93E-01	6.33E-02
19	342.5	1.80	4541		400	1716	2.76E-01	9.11E-02
20	345.0	2.30	5803		410	908	3.64E-01	1.20E-01
21	347.5	2.70	6812					days-1
22	350.0	2.60	6560					hrs-1
23	352.5	2.50	6308				ϕ =	1.00E-03
24	355.0	2.60	6560				$\tau_{0.5}$(hrs) =	
25	357.5	2.70	6812					
26	360.0	2.80	7064					
27	362.5	2.80	7064					
28	365.0	2.70	6812					
29	367.5	2.70	6812					
30	370.0	2.70	6812					
31	372.5	2.70	6812					
32	375.0	2.60	6560					
33	377.5	2.60	6560					
34	380.0	2.60	6560					
35	382.5	2.80	7064					
36	385.0	2.90	7317					
37	387.5	2.80	7064					
38	390.0	2.40	6055					
39	392.5	1.70	4289					
40	395.0	1.20	3028					
41	397.5	0.70	1766					
42	400.0	0.30	757					
43	402.5	0.50	1262					
44	405.0	0.70	1766					
45	407.5	0.50	1262					
46	410.0	0.30	757					
47	412.5	0.20	505					
48	415.0	0.10	252					

Concawe
Environmental Science
for European Refining

Concawe
Boulevard du Souverain 165
B-1160 Brussels
Belgium

Tel: +32-2-566 91 60
Fax: +32-2-566 91 81
e-mail: info@concawe.org
http://www.concawe.eu

ISBN 978-2-87567-127-1